



# An innovative process for dealkalization of red mud using leachate from Mn-containing waste

Zehai Li<sup>a,c</sup>, Hannian Gu<sup>b,c,\*</sup>, Bing Hong<sup>a</sup>, Ning Wang<sup>b</sup>, Mengjun Chen<sup>d</sup>

<sup>a</sup> State Key Laboratory of Environmental Geochemistry, Institute of Geochemistry, Chinese Academy of Sciences, Guiyang 550081, China

<sup>b</sup> Key Laboratory of High-Temperature and High-Pressure Study of the Earth's Interior, Institute of Geochemistry, Chinese Academy of Sciences, Guiyang 550081, China

<sup>c</sup> University of Chinese Academy of Sciences, Beijing 100049, China

<sup>d</sup> Key Laboratory of Solid Waste Treatment and Resource Recycle, Ministry of Education, Southwest University of Science and Technology, Mianyang 621010, China

## ARTICLE INFO

Editor: Fumitake Takahashi

### Keywords:

Red mud

Dealkalization

Mn-containing leachate

Multistage

Disposal waste with waste

## ABSTRACT

Red mud (RM) is an alkaline industrial solid waste discharged from Bayer process, and its high alkalinity is considered as a serious influence on environment and application. Dealkalization is prerequisite and basis for the complete utilization of RM. Mn-containing leachate is a weakly acidic wastewater generated during the storage of manganese sulfate residue. In the current study, Mn-containing leachate was used to investigate the multistage dealkalization behavior of RM. The results showed that Mn-containing leachate effectively lowered pH levels from 11.82 to 7.61 and the leaching efficiency of Na and K reached 80% and 73%, respectively, under the conditions of five-stage leaching with reaction temperature of 95 °C, reaction time of 2.0 h, and a liquid-solid ratio of 10 mL/g. X-ray fluorescence spectrometer analysis results suggested that the content of sodium oxide was reduced from 4.97% to 0.78% while the contents of SiO<sub>2</sub>, Al<sub>2</sub>O<sub>3</sub> and Fe<sub>2</sub>O<sub>3</sub> were essentially unchanged. X-ray photoelectron spectrometer and X-ray diffraction analysis revealed that hydroxycancrinite in RM was dissolved accompanying sodium released and Mn(II) appeared in the newly-generated form of charmatite in the dealkalized RM. The final dealkalized RM product was demonstrated to be with low soluble heavy metals from its water leaching test. This research provides a sustainable reference of disposal waste with waste for the dealkalization of RM, and the findings of this work demonstrate a new mechanism of replacement Na with Mn in RM dealkalization process.

## 1. Introduction

Red mud (RM), also known as bauxite residue, is an alkaline solid waste by-product derived in the extraction process of alumina from bauxite ore. With increasing demands for alumina, the global reserves of RM have reached 4.6 billion tons in 2018, and it is estimated that an annual increase was approximately 200 million tons [1]. The treatment and disposal of RM has been posing a huge challenge for alumina plants and the alumina industry, and the improper storage in bauxite residue disposal areas (BRDAs) can easily cause significant problems leading to environmental threats. In the downwind area of BRDAs, soil alkalinity is induced and heavy metals from RM can be transferred with the dust resulting in high concentrations distribution in the surrounding soil [2]. There are also several reports on contaminations/accidents issues caused by the discharge of high pH residue leachate [3–5]. Many efforts

have been made to find cost-efficient and sustainable applications including construction materials, production of ceramics, environmental adsorbents [6–9], and secondary source for metals recovery [10]. However, in addition to the small quantity of consumption, the high alkalinity of RM is an important and intractable obstacle which restricts its bulk application in the existing fields of soil aggregates and building materials [11–14].

The high alkali contents and high pH values of RM are ubiquitous because bauxite is digested in a hot NaOH solution [11,15]. Due to the high alkaline nature, it is possible to use RM for preparing alkali-activated materials or geopolymer [8]. On the other hand, in most cases for RM applications, neutralization to lower the initial pH and conversion of alkaline characteristics are necessary [16,17]. Utilizing as building materials is one of the main ways to consume RM in large quantities. For applications in building materials, in addition to

\* Corresponding author at: Key Laboratory of High-Temperature and High-Pressure Study of the Earth's Interior, Institute of Geochemistry, Chinese Academy of Sciences, Guiyang 550081, China.

E-mail address: [guhannian@vip.gyig.ac.cn](mailto:guhannian@vip.gyig.ac.cn) (H. Gu).

<https://doi.org/10.1016/j.jece.2022.107222>

Received 14 September 2021; Received in revised form 24 December 2021; Accepted 15 January 2022

Available online 18 January 2022

2213-3437/© 2022 Elsevier Ltd. All rights reserved.

reducing the pH of the RM, the sodium content must be less than 1% due to low strength [13,18] and inadequate durability caused by alkali efflorescence phenomenon [19]. Therefore, dealkalization is a prerequisite and basis for the complete utilization of RM.

In general, the alkaline substances of RM can be mainly classified into soluble alkali and sparingly soluble structural alkali [1,20]. In recent studies, the main dealkalization methods for RM were summarized as follows: acid leaching, acid gas sequestration, salt precipitation or ion replacement, and waste by-product leaching [20,21]. Acid leaching mainly involves using mineral acids and organic acids [13,17,22], and acid leaching process also focuses on the secondary recovery of valuable metals [23]. However, strong acid leaching will also cause dissolution of silicon, aluminum and iron in RM, which tend to form colloids leading to difficulties for subsequent solid-liquid separation [20]. Furthermore, the yields of dealkalized RM are reduced [24], and the dealkalized products are acidic and are adverse to follow-up applications [20]. Carbon dioxide and other industrial exhausts have been validated to be of significance to RM neutralization with consumption of acid gases [12]. The method is sustainable due to disposal waste with waste, and it is included in the category of acid neutralization in a recent review publication [20]. Seawater/brine neutralization and gypsum remediation are based on the process of salt precipitation or ion replacement. Specifically, the mechanism of seawater and brine neutralization is the formation of hydrotalcite through the reaction of  $\text{Ca}^{2+}$  and  $\text{Mg}^{2+}$  precipitated alkaline anions, thereby reducing the pH value [25]. However, these methods need high liquid-solid ratio and are not available to industries in non-coastal areas. Gypsum is a slightly soluble calcium salt, and blending gypsum with RM can continuously release calcium ions to precipitate the alkaline anions through calcium and sodium replacement [26,27]. Owing to gypsum's slow dissolution rate and limitation of in situ application for RM [28], it is difficult to widely apply gypsum remediation or neutralization [29]. Consequently, dealkalization or neutralization treatment of RM should be economical and effective.

Manganese-bearing ores are extracted using sulfuric acid to obtain manganese sulfate product. Manganese sulfate residue (MSR) is discharged as a kind of industrial waste during the process of filtration and separation from the sulfuric acid leaching pulp [30]. The stockpile area of MSR would generate Mn-containing leachates. It is difficult to dispose of the Mn-containing leachates because impurities inside are relatively high and the low concentration of manganese is not expected to be recycled by mixing with the high-concentration manganese sulfate solution in the production line. In the current study, RM was leached using the mentioned Mn-containing leachate to reduce its sodium and potassium to meet the application requirements. The dealkalization efficiency of using Mn-containing leachate was compared with of using a prepared  $\text{MnSO}_4$  solution, and then the main experimental factors using Mn-containing leachate, including leaching temperature, leaching time and liquid-solid ratio, were investigated. In addition, the reaction mechanism referring to sodium releasing and manganese solidifying was discussed. The findings of this study provide a theoretical support for dealkalization treatment of RM using manganese ions and make the concept of disposal waste with waste be feasible in practical applications.

## 2. Material and methods

### 2.1. Materials and leachate preparation

The RM sample used was fresh and collected from the conveyor belt discharging to the disposal areas in an alumina refinery in Qingzhen, Guizhou Province of China. The main chemical and phase compositions of the RM were determined, and as reported elsewhere [31] the main chemical components in RM were  $\text{Al}_2\text{O}_3$  (21.54%),  $\text{Fe}_2\text{O}_3$  (18.43%),  $\text{CaO}$  (15.20%),  $\text{Na}_2\text{O}$  (4.97%),  $\text{K}_2\text{O}$  (1.04%) and  $\text{SiO}_2$  (16.69%).

Manganese sulfate residue was newly discharged in stockpiling site

in a manganese sulfate production enterprise in Tongren, Guizhou Province of China. Raw samples of RM and MSR were dried at 80 °C for 24 h in a drying oven (WGL-125B) and were subsequently ground into fine powders using a mortar and pestle, and then sieved over a 150  $\mu\text{m}$  stainless-steel mesh. To determine the soluble manganese sulfate that MSR contained, the dried and screened MSR was mixed with deionized water under the condition of room temperature of 25 °C with a liquid-solid ratio of 10 mL/g. After reaction for 2 h, Mn-containing solution from MSR was collected through filtration with a vacuum suction filter. The simulated Mn-containing solution obtained here was regarded as a substitution leachate, which derived from the stock dump of MSR. The main elemental concentration of the Mn-containing leachate is given in Table 1, and the pH value was measured to be 6.02. The results showed that Mn, S, Ca, and Na were the main elements in the Mn-containing leachate and the concentration of Mn was as high as 3050 mg/L.

Since  $\text{Mn}^{2+}$  and  $\text{SO}_4^{2-}$  were the main composition in the Mn-containing leachate (as shown in Table 1), laboratory-made  $\text{MnSO}_4$  solution (3000 mg Mn/L) was performed as a contrast for RM dealkalization experiments. The prepared  $\text{MnSO}_4$  solution was determined with a pH value of 6.43, slightly higher than the Mn-containing leachate. Manganese sulfate monohydrate of analytical grade (Tianjin Kemiou Chemical Reagent Co., Ltd) was used to prepare  $\text{MnSO}_4$  solutions. All solutions/leachates in this study were prepared with deionized water.

### 2.2. Leaching experiment

RM dealkalization using Mn-containing leachate in the current study was realized through batch leaching tests. A five-stage leaching was performed for all experimental trials. After each stage leaching experiment, the filtration residue was washed with deionized water for 3 times, while the leaching and washing solutions were mixed for determination. The washed filtration residue was then used for the next leaching stage by adding corresponding volume of Mn-containing leachate until five stages were performed.

All leaching experiments were performed in a thermostatic water bath (THZ-82A) mechanically stirred at a speed of 240 rpm, and 5.0 g of prepared RM sample was used in each experimental trial to react with Mn-containing leachate in a conical flask covered with a piece of polyethylene plastic membrane to avoid external interference. Na and K leaching efficiencies on different conditions of leaching temperature, reaction time and liquid-solid ratio were investigated: (1) For confirming the suitable leaching temperature, the dried and sieved RM was leached with 50 mL Mn-containing leachate at temperatures of 20, 40, 80, 90 and 95 °C for a period of 2 h. (2) For reaction duration investigation, reaction time was controlled for 1.0, 1.5 and 2.0 h using a liquid-solid ratio of 10 mL/g at 95 °C. (3) In the liquid-solid ratio trials, leaching reactions using different liquid-solid ratios of 5, 10, and 15 mL/g were carried out for 2.0 h at 95 °C.

To determine the pH of original RM and MSR, both samples were mixed with deionized water (5.0 g of sample with 50 mL water), and the slurries were filtered after shaking for 8 h. The obtained solutions were measured using a pH meter (pHS-SC). The pH value of the final leachate was measured to represent the pH of the final dealkalized RM. To investigate the release of manganese and other metals in the original RM and the final dealkalized RM, 3.0 g of each dried sample was added into 30 mL deionized water for leaching reaction at room temperature for 2 h. After reaction the leachate was separated for determination.

All leaching experiments for RM dealkalization were carried out three times for assuring data accuracy, and the results are expressed as mean and standard deviation (seen in Table S1). The concentrations of Na, K, Al, Ca, Fe, Mg and Si in each leaching solution were then determined to estimate the leaching efficiency. The dealkalization and leaching efficiency of Na and K from the RM in this study was calculated as Eq. (1).

**Table 1**  
Main elemental concentrations of Mn-containing leachate (mg/L).

Element	Mn	S	Ca	Na	Mg	K	Si	Al	Fe
Concentration	3050	2290	330	131.0	41.7	35.7	3.4	0.57	0.18

$$X = \frac{c_1V_1 - c_2V_2}{m \times 1000 \times w} \times 100\% \quad (1)$$

where  $X$  (%) represents leaching efficiency of element (including Na, K, Al, Ca, Fe, Mg and Si) from the original RM;  $c_1$  (mg/L) and  $c_2$  (mg/L) are the concentrations of the above element in the leaching solution and the Mn-containing leachate used, respectively;  $V_1$  (L) and  $V_2$  (L) are the volumes of the leaching solution and the Mn-containing leachate used, respectively;  $m$  (g) is the mass of the original RM;  $w$  (%) is the content of the above element in the original RM.

### 2.3. Characterization methods

Original RM sample and the dealkalinized RM samples were characterized by X-ray diffraction (XRD, PANalytical Empyrean) with Cu K $\alpha$  radiation conducted with a 2 $\theta$  scan range from 5° to 70°. Jade 6.0 was used to analyze the mineral phase difference of the RM and the dealkalinized RM samples. The original RM and the dealkalinized RM obtained under the conditions of five-stage leaching with reaction temperature of 95 °C, reaction time of 2.0 h, and a liquid-solid ratio of 10 mL/g, were also characterized as follow. The main chemical compositions of the original RM and the dealkalinized RM were determined using X-Ray Fluorescence Spectrometer (XRF, PANalytical PW2424). The morphology and microstructure of the samples was viewed in a scanning electron microscope (SEM, FEI Scios). Surface elements compositions of the original RM and the dealkalinized RM were determined by X-ray photoelectron spectrometer (XPS, ThermoFisher, Thermo Scientific K-Alpha+) with a monochromatic Al K $\alpha$  (1486.6 eV) X-ray source. The measurements were carried out at a work power of 15 kV and beam current of 15 mA at a vacuum of  $5 \times 10^{-9}$  mbar. The 284.8 eV value of the hydrocarbon C1 core level was used as a calibration for the absolute energy level.

The concentrations of Na, K, Al, Ca, Fe, Mg and Si in the original Mn-containing leachate and each leaching solution were determined by inductively coupled plasma-optical emission spectroscopy (ICP-OES, Varian VISTA).

## 3. Results and discussion

### 3.1. Leaching efficiency of the Mn-containing leachate and MnSO<sub>4</sub> solution

As has been widely recognized, different RM samples have a wide range of variation in the main chemical compositions, and are with complex mineral compositions [11,23,31]. According to the XRD analysis (Fig. S1), the main mineral phases of the original RM in this study were hydroxycancrinite, katoite, hematite, anatase, chamosite and calcite. Alkali existed as hydroxycancrinite in RM was sparingly soluble and difficult to be removed [16]. Each RM sample was leached for 5 stages using Mn-containing leachate at 95 °C for 2 h with a liquid-solid ratio of 10 mL/g. The effect of each leaching stage on dealkalinization efficiency is shown in Fig. 1. The results showed that the Na leaching efficiency could reach 36% at the first stage, and then it decreased to 13%, 11%, 10% and 8.8% at the following four stages. The total Na leaching efficiency achieved 80% as shown in inset in Fig. 1a. The Na leaching efficiency dramatically declined from the second leaching stage. The finding suggested that the first leaching stage played an important role in leaching process. This can be explained by the fact that RM contained 20–25% soluble chemical alkalis which were easy to be removed at the first stage [20,23,32]. The decline of Na leaching

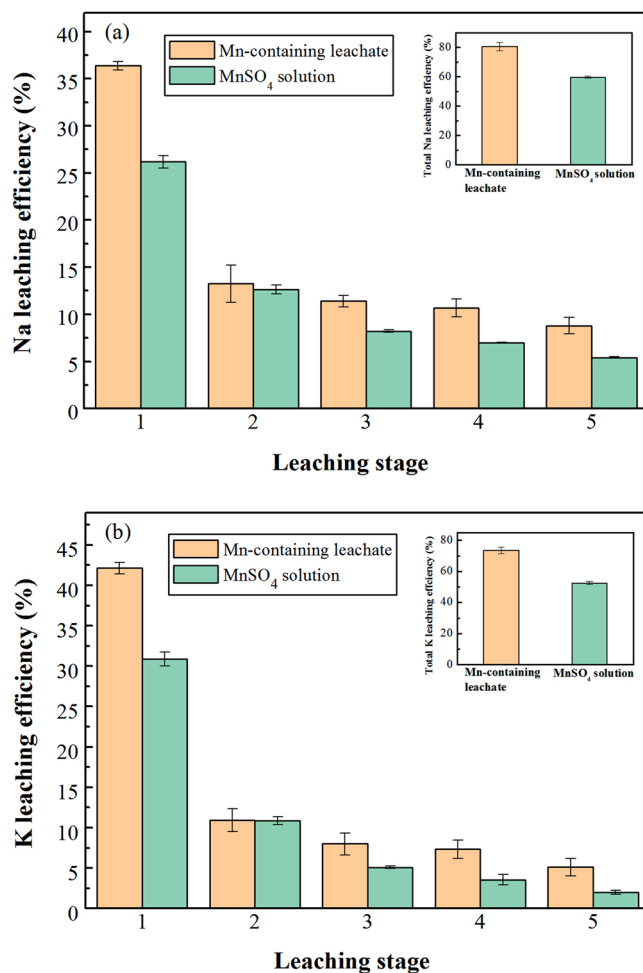


**Fig. 1.** Effects of leaching stage on (a) sodium and (b) potassium leaching efficiency from RM using Mn-containing leachate and MnSO<sub>4</sub> solution (at 95 °C for 2 h with a liquid-solid ratio of 10 mL/g).

efficiency was slight in the following leaching stages, and the results were consistent with the previous literature [16]. Additionally, the leaching behavior of sodium and potassium presented a similar pattern as shown in Fig. 1b, and the total K leaching efficiency could reach 73% (inset in Fig. 1b).

In contrast, the prepared MnSO<sub>4</sub> solution with a Mn<sup>2+</sup> concentration of 3000 mg/L was used to investigate the Na and K leaching efficiency at the same conditions (95 °C, 2 h, and a liquid-solid ratio of 10 mL/g), and the results are contrasted in Fig. 1. The MnSO<sub>4</sub> solution exhibited a lower leaching efficiency of sodium and potassium at each stage. As mentioned, the acidity of prepared MnSO<sub>4</sub> solution (pH 6.43) was slightly weaker than that of the Mn-containing leachate (pH 6.02). The pH distinction might be explained by hydrolysis induced by other cations that the Mn-containing leachate contained, and it is also probable that the acidic manganese sulfate residue resulted in a lower pH for the Mn-containing leachate. High hydron concentration can promote dissolution of Ca in red mud as calcite [13], and Ca can reduce pH and replace the exchangeable Na [14,33]. Due to these reasons, the MnSO<sub>4</sub> solution did not reach the corresponding leaching efficiency as the

Mn-containing leachate, especially at the first stage. As a result, the total leaching efficiency of sodium and potassium was 60% and 52%, respectively, and the leaching efficiencies could not meet the requirements for RM dealkalization, which needed less than 1% of sodium content [13]. Since the Mn-containing leachate was more efficient than  $\text{MnSO}_4$  solution, the Mn-containing leachate was then used for effect factor investigation in the following leaching process of RM dealkalization.

### 3.2. Effect of leaching temperature

The effect of leaching temperature on dealkalization efficiency using the Mn-containing leachate was investigated under the condition of leaching time of 2 h and liquid-solid ratio of 10 mL/g, and the results are depicted in Fig. 2. It can be observed from the curves that the leaching efficiency of Na and K increased with the increasing of leaching temperature. At room temperature of 20 °C, the leaching efficiency of Na and K was 17% and 20%, respectively, whereas it reached 80% and 73% when the leaching temperature increased at 95 °C. The results indicated that higher temperature could provide the reaction activity and that increasing the leaching temperature was beneficial for enhancing the dissolution of alkali substances to release Na and K. In the hydrometallurgy processing for alkali removal from RM, as reported, leaching temperature of 90 °C or higher was selected as suitable conditions [12, 16]. Therefore, 95 °C was selected as the suitable leaching temperature in this experiment.

The high pH is an inhibitor due to the potentially adverse effects in the particular application [34,35], thus the final pH was the one of the main parameters for dealkalized RM [36]. To evaluate the efficiency of Mn-containing leachate on alkalinity of RM, the final pH values for the leaching solution at different leaching temperature were determined and the results are displayed in Fig. S2. With controlling leaching temperature at 20 °C, an obvious decrease in final pH (from 11.82 to 7.97) was obtained. It can be inferred that the neutralization reaction occurred at this period was mainly attributed to the dissolution of free alkali. As the leaching temperature increased, the final pH decreased gradually and slightly (from 7.97 to 7.61), which indicated that the leaching reaction was mild and the Mn-containing leachate would not lead to acidic dealkalized-RM products even though the dealkalization efficiency reached 80%.

Silicon, aluminum and iron were subjected to dissolution resulting in dealkalized solid product reduced when using mineral acids for RM dealkalization. Moreover, the process consumes large amounts of acids and brings difficulties to filtration [20,24]. In this study, when the dealkalization efficiency reached 80% at the condition of leaching

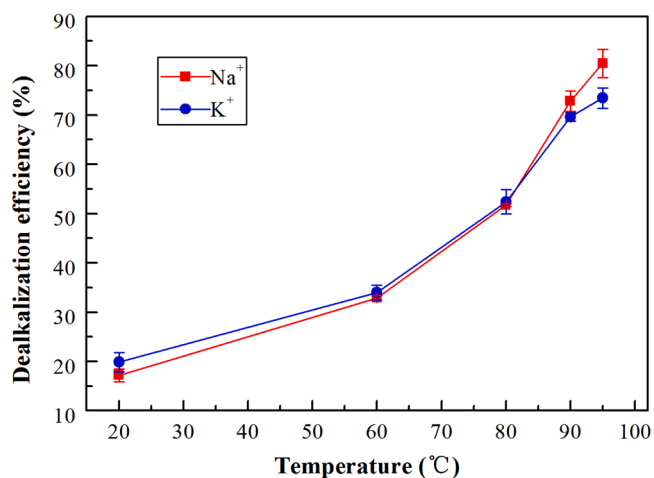


Fig. 2. Effect of leaching temperature on dealkalization efficiency from RM using Mn-containing leachate (for 2 h with a liquid-solid ratio of 10 mL/g).

temperature 95 °C, leaching time 2 h with 5 stages, and liquid-solid ratio 10 mL/g, the leaching amounts of silicon, aluminum and iron from RM was no more than 1% (Table 2). It is an advantage for using Mn-containing leachate for RM dealkalization.

### 3.3. Effect of leaching time and liquid-solid ratio

The leaching experiments using the Mn-containing leachate were performed under the condition of liquid-solid ratio of 10 mL/g at 95 °C, to further investigate the effect of reaction time on the Na and K leaching efficiencies from RM. In the process of Na dissolution or leaching, generally, the contact time for waste liquor leaching [21] was longer than for acid leaching [13]. The reaction time of each stage was set as 1.0, 1.5 and 2.0 h, and the results are shown in Fig. 3. The results suggested that the leaching efficiencies of Na and K from RM increased simultaneously with increasing reaction time. When the reaction time was increased from 1.0 h to 2.0 h, the Na and K leaching efficiencies increased from 61% to 80% and from 60% to 73%, respectively. Leaching duration set as 2.0 h was not long for RM dealkalization and has been accepted in acid-free leaching methods, for example, Rai et al. [21] reported 135 min as suitable time when using acidic pickling waste liquor for RM neutralization of alkaline. Hence, the suitable reaction time was 2.0 h.

The Mn-containing leachate leaching experiments for the effect of liquid-solid ratios investigation were conducted under the conditions of leaching temperature of 95 °C and reaction time of 2 h, and the results are shown in Fig. 4. The leaching trend of the Na and K was similar with the increasing of liquid-solid ratio as shown in Fig. 4. With the liquid-solid ratio increased from 5 to 10 mL/g, the leaching efficiencies of Na and K increased from 59% to 80% and from 56% to 73%, respectively. With the liquid-solid ratio changed from 10 to 15 mL/g, the leaching efficiencies of Na and K continued to increase from 80% to 89% and from 73% to 78%, respectively. This suggested that improving the liquid-solid ratio meant larger volumes of the solutions which accelerated the mass transfer and diffusion of reactants during the Mn-containing leachate leaching process. However, the liquid-solid ratio for the dealkalization process cannot be as high as possible for higher liquid-solid ratios would generate larger volumes of leached solutions which needed an appropriate follow-up processing. Wang et al. [12] reported a liquid-solid ratio of 5 mL/g for RM dealkalization by adding carbide slag, which depends on the reactant and the Na content of RM. In terms of RM used in this study, 10 mL/g was selected as the suitable liquid-solid ratio. In this condition, the processed RM with less than 1% of sodium content could meet the demand of application for construction materials [13,18].

### 3.4. Mechanism analysis on dealkalization process

The Mn-containing leachate mainly contained manganese ion and sulfate, and Mn ion was thought to replace the structural Na of alkaline substances in RM. The following characterization validated the conception.

Table 2

Leaching efficiency of Al, Ca, Fe, Mg and Si from RM using Mn-containing leachate at different leaching temperatures under the condition of the reaction time of 2 h with a liquid-solid ratio of 10 mL/g (wt%).

Temperature (°C)	Al	Ca	Fe	Mg	Si
20	0.04	7.54	0.01	4.86	0.15
60	0.04	12.73	0.01	5.14	0.32
80	0.05	16.22	0.01	6.01	0.67
90	0.05	23.61	0.01	17.01	0.88
95	0.06	23.82	0.01	18.03	1.00

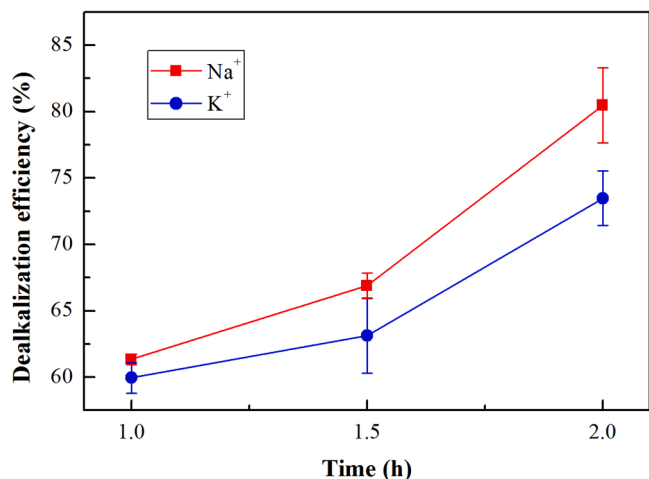


Fig. 3. Effect of reaction time on dealkalinization efficiency from RM using Mn-containing (at 95 °C with a liquid-solid ratio of 10 mL/g).

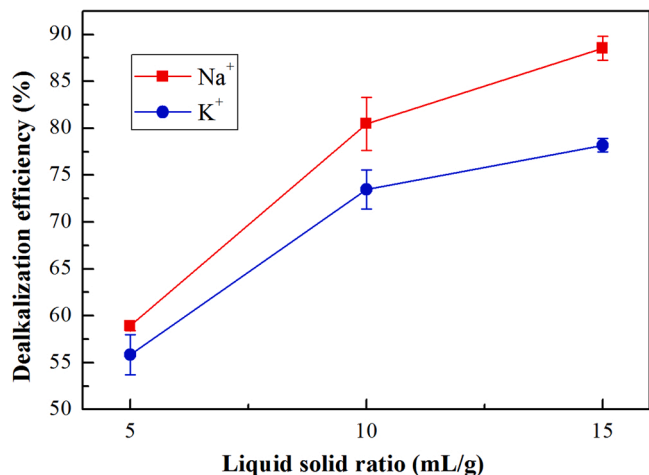


Fig. 4. Effect of liquid-solid ratio on dealkalinization efficiency from RM using Mn-containing leachate (at 95 °C for 2 h).

### 3.4.1. XPS analysis results

To further reveal the mechanism of dealkalinization process, XPS analyses were conducted to compare the surface chemical state of

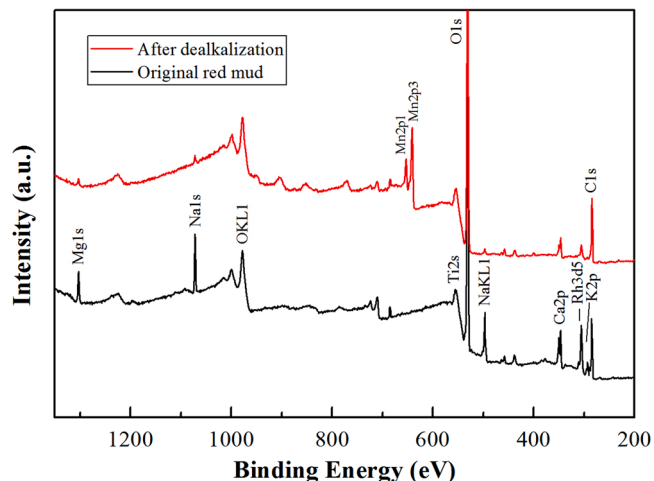


Fig. 5. XPS high resolution spectra of the original RM, and the dealkalinized RM.

dealkalinized RM and the original RM obtained under the suitable conditions of 95 °C, 2.0 h, and 10 mL/g. Fig. 5 illustrates the whole region scans of the original RM and the dealkalinized RM. It can be seen that the XPS peaks with Mg 1s, Na 1s (Na Auger), and K 2p with corresponding binding energies at 1303.3, 1072.0 (497.3), and 293.6 eV, respectively, could be recognized from the original RM spectrum. These characteristic peaks obviously became weak at the dealkalinized RM spectrum, indicating that Mg, Na and K were effectively removed during the leaching process using Mn-containing leachate. On the other hand, the binding energy positions of ~641 eV (Mn 2p<sub>3/2</sub>) and ~653 eV (Mn 2p<sub>1/2</sub>) at the dealkalinized RM spectrum were observed, which can basically be attributed to the presence of Mn(II) compounds [37,38]. The newly-generated peaks in comparison to the original RM implied that Mn precipitated in the dealkalinized RM during the dealkalinization process.

### 3.4.2. XRD and SEM analysis

The main mineral phases of the original RM sample and the dealkalinized products at different dealkalinization temperatures are shown in Fig. 6. By a contrastive analysis with original RM, the main mineral phases in processed RM products were basically unchanged, embodied in aluminosilicates such as katoite and chamosite (Fig. 6). Katoite was reported to be present in RM samples as calcium aluminate hydrates [39], which was stable and would not change during leaching process [40]. As one of silicate minerals, chamosite can be partially digested during autoclave digestion and decomposition [41]. The small amounts of Ca, Al and Si were released (Table 2) during the leaching process, which are also consistent with the XRD results. In addition, layered structures and smooth surfaces of aluminosilicates were observed in both of the original and the dealkalinized RM product obtained using Mn-containing leachate at leaching temperature of 95 °C for 2 h with 10 mL/g as shown in Fig. 7. The results indicate that the dealkalinization process was mild so as to maintain their micro morphologies.

However, Na-containing phase disappeared and Mn-containing phases generated during the leaching process in this study as shown in Fig. 6. Cancrinite is one of the major existing forms of sodium in RM [42–44], and it cannot be water leached for it belongs to structural alkalis (chemical bonded alkalis) [16,42]. Cancrinite can be dissolved accompanied by generating hydroxycancrinite in seawater neutralized RM process [25], while in the pyrometallurgical method for RM dealkalinization it decomposed into carbonate and aluminosilicates [16]. As a cancrinite-subgroup mineral, hydroxycancrinite [(NaAl-SiO<sub>4</sub>)<sub>6</sub>·2NaOH·2H<sub>2</sub>O] is also presented in some RM samples [23,44,45], which can only form in low CO<sub>2</sub> system [46]. In the current study, when the reaction temperature increased, peaks of hydroxycancrinite tended to be weaker and there was no appearance of the peaks at leaching

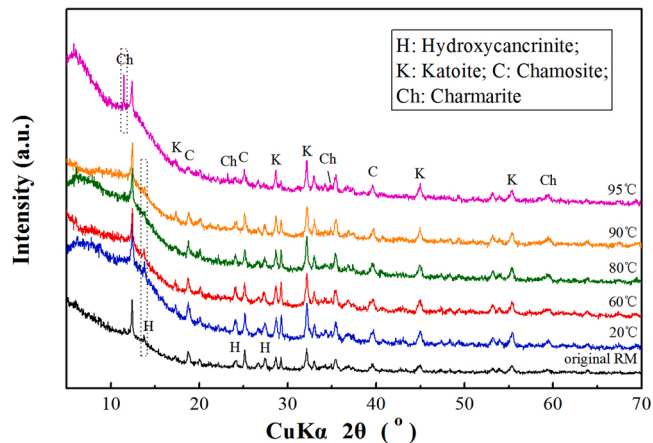


Fig. 6. XRD patterns of the original RM and the dealkalinized RM products obtained at leaching temperature of 20, 60, 80, 90 and 95 °C (with 10 mL/g for 2 h).

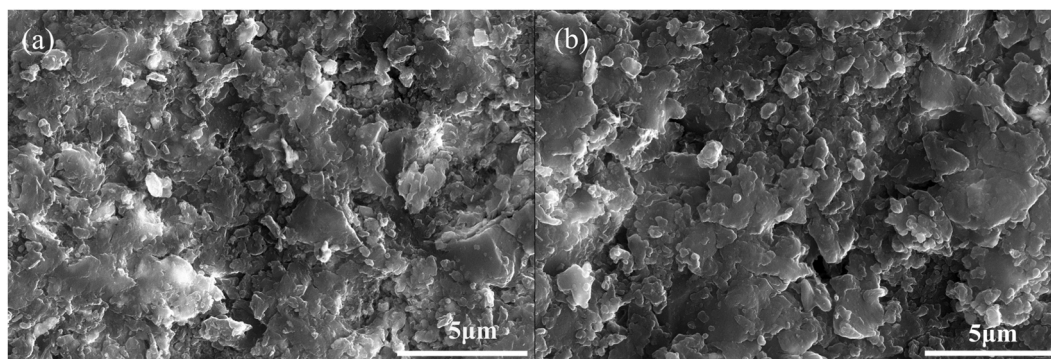
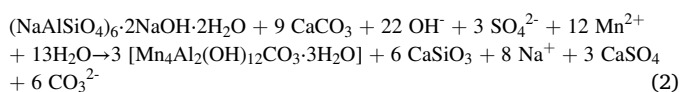


Fig. 7. SEM analysis of (a) the original RM, and (b) the dealkalized RM product.

temperature of 95 °C. Whereas, charmarite  $[\text{Mn}_4\text{Al}_2(\text{OH})_{12}\text{CO}_3 \cdot 3\text{H}_2\text{O}]$  was observed as a newly generated phase, implying that Mn ions solidification took place through the replacement of Na in alkaline substances since charmarite was considered to be a typical hydrate with high hardness [47]. These results indicate that hydroxycancrinite as the main structural alkali in RM has transformed into charmarite. Based on the above analysis, the main chemical reaction might be summarized as Eq. (2):



In combination with XRD patterns, Eq. (2) only provided the main possible dissolution reaction between Na-containing substances and Mn ions, and other similar dissolution reactions might also exist: for example, the acidity of Mn-containing leachate caused Ca dissolution (Table 2), which could replace the exchangeable Na. The alkaline substances such as calcite and cancrinite in RM would form a pH buffer through their dissolution reactions, resulting in pH rebounding [20,48]. In this study, multistage leaching using Mn-containing leachate introduced abundant Mn ions and promoted the alkaline substances consumption.

The multistage reactions might occur progressively when leaching temperature reached 95 °C. In terms of at the lower leaching temperatures, the dealkalization process might mainly attribute to the release of free alkali, such as NaOH,  $\text{Na}_2\text{CO}_3$ ,  $\text{NaHCO}_3$ , and  $\text{Na}[\text{Al}(\text{OH})_4]$ . Leachate with Mn ions can also reduce the alkaline anions by precipitating such as  $\text{OH}^-$  and  $[\text{Al}(\text{OH})_4]^-$  if their concentrations are large enough.

### 3.5. Characteristics of the dealkalized RM

The dealkalized RM obtained under the suitable conditions of 95 °C, 2.0 h, and 10 mL/g was characterized including composition analysis and water-leaching tests. The chemical composition of the dealkalized RM was determined by XRF, and the data are shown in Table 3. Compared with the original RM, the composition of the leaching residue after dealkalization did not change obviously except for sodium, potassium and manganese. The findings also demonstrated that the yields of dealkalized RM (Table S2) in this study were not reduced in comparison with dealkalization using mineral acids. The reserved compositions of alumina and silica are valid components when using as building material additives. The sodium oxide content decreased from

4.97% to 0.78%, which makes it possible to meet the demand of application for construction materials [13]. As discussed above, manganese in the dealkalized RM was mainly presented in charmarite which is beneficial for application in building materials [47].

To investigate the release of manganese and other metals, 3.0 g of the original/dealkalized RM was leached with 30 mL deionized water under the conditions of room temperature for 2 h. Table 4 presents the metal concentrations of the water leaching solutions. It can be inferred that the concentrations of manganese and the other metals are low. The low concentration of manganese is in agreement with the formation of charmarite that can consume Mn ions. In conclusion, the Mn-containing leachate used in this study could not only effectively reduce the alkalinity of RM, but also maintain the dealkalized RM feasibility for subsequent treatment. More importantly, the Mn-containing leachate would be cost less for it was from industrial waste.

## 4. Conclusions

The current work presented a sustainable new technology to dealkalize RM, which was based on using leachate from Mn-containing waste. When the dealkalization process was under the condition of leaching temperature of 95 °C, reaction time of 2.0 h, five-stage leaching, liquid to solid ratio of 10 mL/g, the Na and K leaching efficiencies reached 80% and 73%, respectively, with pH being reduced from 11.82 to 7.61. The content of sodium oxide in dealkalized RM was reduced from 4.97% to 0.78%. Meanwhile, the contents of other components including silicon, aluminum and iron oxides were less reduced, which was conducive to the subsequent applications. The introduced manganese ions were thought to replace sodium in hydroxycancrinite and to form a stable Mn-containing phase, charmatite, which was acceptable for environment. Limited release of soluble heavy metals from the dealkalized RM product was found following leaching tests. The findings of this research provided a basic train of thought of disposal waste with waste for dealkalization of RM.

### CRediT authorship contribution statement

**Zehai Li:** Investigation, Resources, Data curation, Writing – original draft. **Hannian Gu:** Writing – review & editing, Conceptualization, Methodology, Supervision, Funding acquisition. **Bing Hong:** Supervision. **Ning Wang:** Conceptualization, Supervision. **Mengjun Chen:** Resources.

Table 3

Main chemical compositions of the original RM and the dealkalized RM leached by Mn-containing leachate (wt%).

Sample	$\text{Al}_2\text{O}_3$	CaO	$\text{Fe}_2\text{O}_3^a$	$\text{K}_2\text{O}$	MgO	MnO	$\text{Na}_2\text{O}$	$\text{P}_2\text{O}_5$	$\text{SiO}_2$	$\text{SO}_3$	$\text{TiO}_2$	LOI
original RM	21.54	15.20	18.43	1.04	1.62	0.03	4.97	0.37	16.69	1.04	4.71	11.30
dealkalized RM	20.32	11.60	18.00	0.54	1.42	11.15	0.78	0.39	16.28	2.32	4.83	12.30

<sup>a</sup> Annotation: results of  $\text{Fe}_2\text{O}_3$  were obtained from ICP-OES.

Table 4

Metal elements concentration of the water leaching solution from the original RM and the dealkalized RM leached by Mn-containing leachate (mg/L).

Element	As	Al	Ba	Hg	Cd	Cu	Fe	Pb	Mn	Zn
original RM	< 0.01	19.45	< 0.01	< 0.02	< 0.01	< 0.01	< 0.01	< 0.02	< 0.01	< 0.01
dealkalized RM	< 0.01	0.17	< 0.01	< 0.02	< 0.01	< 0.01	< 0.01	< 0.02	8.11	< 0.01

### Declaration of Competing Interest

The authors declare that they have no known competing financial interests or personal relationships that could have appeared to influence the work reported in this paper.

### Acknowledgments

The work was financially supported by the National Key Research and Development Program of China (2018YFC1903500), the National Natural Science Foundation of China (U1812402), and The Youth Innovation Promotion Association CAS (No. 2021400).

### Appendix A. Supporting information

Supplementary data associated with this article can be found in the online version at [doi:10.1016/j.jece.2022.107222](https://doi.org/10.1016/j.jece.2022.107222).

### References

- S. Xue, Y. Wu, Y. Li, X. Kong, F. Zhu, W. Hartley, X. Li, Y. Ye, Industrial wastes applications for alkalinity regulation in bauxite residue: a comprehensive review, *J. Cent. South Univ.* 26 (2019) 268–288, <https://doi.org/10.1007/s11771-019-4000-3>.
- J. Ren, J. Chen, L. Han, M. Wang, B. Yang, P. Du, F. Li, Spatial distribution of heavy metals, salinity and alkalinity in soils around bauxite residue disposal area, *Sci. Total Environ.* 628–629 (2018) 1200–1208, <https://doi.org/10.1016/j.scitotenv.2018.02.149>.
- I.T. Burke, C.L. Peacock, C.L. Lockwood, D.I. Stewart, R.J.G. Mortimer, M.B. Ward, P. Renforth, K. Gruiz, W.M. Mayes, Behavior of aluminum, arsenic, and vanadium during the neutralization of red mud leachate by HCl, gypsum, or seawater, *Environ. Sci. Technol.* 47 (2013) 6527–6535, <https://doi.org/10.1021/es4010834>.
- D. Higgins, T. Curtin, R. Courtney, Effectiveness of a constructed wetland for treating alkaline bauxite residue leachate: a 1-year field study, *Environ. Sci. Pollut. Res.* 24 (2017) 8516–8524, <https://doi.org/10.1007/s11356-017-8544-1>.
- J.P. Olszewska, A.A. Meharg, K.V. Heal, M. Carey, I.D.M. Gunn, K.R. Searle, I. J. Winfield, B.M. Spears, Assessing the legacy of red mud pollution in a shallow freshwater lake: arsenic accumulation and speciation in macrophytes, *Environ. Sci. Technol.* 50 (2016) 9044–9052, <https://doi.org/10.1021/acs.est.6b00942>.
- T. Guo, H. Yang, Q. Liu, H. Gu, N. Wang, W. Yu, Y. Dai, Adsorptive removal of phosphate from aqueous solutions using different types of red mud, *Water Sci. Technol.* 2017 (2) (2018) 570–577, <https://doi.org/10.2166/wst.2018.182>.
- R.P. Narayanan, N.K. Kazantzis, M.H. Emmert, Selective process steps for the recovery of scandium from Jamaican bauxite residue (red mud), *ACS Sustain. Chem. Eng.* 6 (2018) 1478–1488, <https://doi.org/10.1021/acssuschemeng.7b03968>.
- X. Chen, Y. Guo, S. Ding, H. Zhang, F. Xia, J. Wang, M. Zhou, Utilization of red mud in geopolymer-based pervious concrete with function of adsorption of heavy metal ions, *J. Clean. Prod.* 207 (2019) 789–800, <https://doi.org/10.1016/j.jclepro.2018.09.263>.
- T. Yang, Y. Wang, L. Sheng, C. He, W. Sun, Q. He, Enhancing Cd(II) sorption by red mud with heat treatment: performance and mechanisms of sorption, *J. Environ. Manag.* 255 (2020), 109866, <https://doi.org/10.1016/j.jenvman.2019.109866>.
- C.R. Borra, B. Blanpain, Y. Pontikes, K. Binnemans, T. Van Gerven, Recovery of rare earths and major metals from bauxite residue (red mud) by alkali roasting, smelting, and leaching, *J. Sustain. Metall.* 3 (2) (2017) 393–404, <https://doi.org/10.1007/s40831-016-0103-3>.
- M. Gräfe, G. Power, C. Klauber, Bauxite residue issues: III. Alkalinity and associated chemistry, *Hydrometallurgy* 108 (2011) 60–79, <https://doi.org/10.1016/j.hydromet.2011.02.004>.
- X. Wang, Y. Zhang, J. Liu, P. Hu, K. Meng, F. Lv, W. Tong, P.K. Chu, Dealkalization of red mud by carbide slag and flue gas, *Clean Soil Air Water* 46 (3) (2018), 1700634, <https://doi.org/10.1002/clen.201700634>.
- G. Hu, F. Lyu, S.A. Khoso, H. Zeng, W. Sun, H. Tang, W. Li, Staged leaching behavior of red mud during dealkalization with mild acid, *Hydrometallurgy* 196 (2020), 105422, <https://doi.org/10.1016/j.hydromet.2020.105422>.
- S. Xue, W. Ke, F. Zhu, Y. Ye, Z. Liu, J. Fan, W. Hartley, Effect of phosphogypsum and poultry manure on aggregate-associated alkaline characteristics in bauxite residue, *J. Environ. Manag.* 256 (2020), 109981, <https://doi.org/10.1016/j.jenvman.2019.109981>.
- H.I. Gomes, W.M. Mayes, M. Rogerson, D.I. Stewart, I.T. Burke, Alkaline residues and the environment: a review of impacts, management practices and opportunities, *J. Clean. Prod.* 112 (2016) 3571–3582, <https://doi.org/10.1016/j.jclepro.2015.09.111>.
- X. Zhu, W. Li, X. Guan, An active dealkalization of red mud with roasting and water leaching, *J. Hazard. Mater.* 286 (2015) 85–91, <https://doi.org/10.1016/j.jhazmat.2014.12.048>.
- X. Kong, M. Li, S. Xue, W. Hartley, C. Chen, C. Wu, X. Li, Y. Li, Acid transformation of bauxite residue: conversion of its alkaline characteristics, *J. Hazard. Mater.* 324 (2017) 382–390, <https://doi.org/10.1016/j.jhazmat.2016.10.073>.
- Y. Wang, T. Zhang, G. Lyu, F. Guo, W. Zhang, Y. Zhang, Recovery of alkali and alumina from bauxite residue (red mud) and complete reuse of the treated residue, *J. Clean. Prod.* 188 (2018) 456–465, <https://doi.org/10.1016/j.jclepro.2018.04.009>.
- S.-P. Kang, S.-J. Kwon, Effects of red mud and alkali-activated slag cement on efflorescence in cement mortar, *Constr. Build. Mater.* 133 (2017) 459–467, <https://doi.org/10.1016/j.conbuildmat.2016.12.123>.
- F. Lyu, Y. Hu, L. Wang, W. Sun, Dealkalization processes of bauxite residue: a comprehensive review, *J. Hazard. Mater.* 403 (2021), 123671, <https://doi.org/10.1016/j.jhazmat.2020.123671>.
- S. Rai, K.L. Wasewar, D.H. Lataye, R.S. Mishra, S.P. Puttewar, M.J. Chaddha, P. Mahindiran, J. Mukhopadhyay, Neutralization of red mud with pickling waste liquor using Taguchi's design of experimental methodology, *Waste Manag. Res.* 30 (2012) 922–930, <https://doi.org/10.1177/0734242X12448518>.
- M.C. Mishra, G.R. Narala, B.H. Rao, Potential of citric acid for treatment of extremely alkaline bauxite residue: effect on geotechnical and geo-environmental properties, *J. Hazard. Toxic Radioact. Waste* 24 (4) (2020), 04020047, [https://doi.org/10.1061/\(ASCE\)HZ.2153-5515.0000541](https://doi.org/10.1061/(ASCE)HZ.2153-5515.0000541).
- S. Rai, K.L. Wasewar, A. Agnihotri, Treatment of alumina refinery waste (red mud) through neutralization techniques: a review, *Waste Manag. Res.* 35 (2017) 563–580, <https://doi.org/10.1177/0734242X17696147>.
- C. Wang, X. Zhang, R. Sun, Y. Cao, Neutralization of red mud using bio-acid generated by hydrothermal carbonization of waste biomass for potential soil application, *J. Clean. Prod.* 271 (2020), 122525, <https://doi.org/10.1016/j.jclepro.2020.122525>.
- S.J. Palmer, R.L. Frost, Characterisation of bauxite and seawater neutralized bauxite residue using XRD and vibrational spectroscopic techniques, *J. Mater. Sci.* 44 (2009) 55–63, <https://doi.org/10.1007/s10853-008-3123-y>.
- R. Haynes, Y. Zhou, Natural ripening with subsequent additions of gypsum and organic matter is key to successful bauxite residue revegetation, *J. Cent. South Univ.* 26 (2019) 289–303, <https://doi.org/10.1007/s11771-019-4001-2>.
- X. Li, Y. Guo, F. Zhu, L. Huang, W. Hartley, Y. Li, X. Kong, S. Xue, Alkalinity stabilization behavior of bauxite residue: Ca-driven regulation characteristics of gypsum, *J. Cent. South Univ.* 26 (2019) 383–392, <https://doi.org/10.1007/s11771-019-4010-1>.
- G. O'Connor, R. Courtney, Constructed wetlands for the treatment of bauxite residue leachate: long term field evidence and implications for management, *Ecol. Eng.* 158 (2020), 106076, <https://doi.org/10.1016/j.ecoleng.2020.106076>.
- R.G. Courtney, S.N. Jordan, T. Harrington, Physico-chemical changes in bauxite residue following application of spent mushroom compost and gypsum, *Land Degrad. Dev.* 20 (2009) 572–581, <https://doi.org/10.1002/ldr.926>.
- S. Ma, H. Gu, Z. Mei, Y. Yang, N. Wang, Conversion of manganese sulfate residue into iron hydroxide adsorbent for Cu(II) removal from aqueous solution, *Environ. Sci. Pollut. Res.* 27 (19) (2020) 23871–23879, <https://doi.org/10.1007/s11356-020-08819-9>.
- H. Gu, N. Wang, J.S.J. Hargreaves, Sequential extraction of valuable trace elements from Bayer process-derived waste red mud samples, *J. Sustain. Metall.* 4 (1) (2018) 147–154, <https://doi.org/10.1007/s40831-018-0164-6>.
- E. Di Carlo, A. Boulemant, R. Courtney, Plant available Al and Na in rehabilitated bauxite residue: a field study assessment, *Environ. Sci. Pollut. Res.* 27 (14) (2020) 17023–17031, <https://doi.org/10.1007/s11356-020-08225-1>.
- D. Higgins, T. Curtin, I. Burke, R. Courtney, The potential for constructed wetland mechanisms to treat alkaline bauxite residue leachate: carbonation and precipitate characterisation, *Environ. Sci. Pollut. Res.* 25 (2018) 29451–29458, <https://doi.org/10.1007/s11356-018-2983-1>.
- K. Evans, The history, challenges, and new developments in the management and use of bauxite residue, *J. Sustain. Metall.* 2 (4) (2016) 316–331, <https://doi.org/10.1007/s40831-016-0060-x>.
- E. Di Carlo, C.R. Chen, R.J. Haynes, I.R. Phillips, R. Courtney, Soil quality and vegetation performance indicators for sustainable rehabilitation of bauxite residue disposal areas: a review, *Soil Res.* 57 (5) (2019) 419–446, <https://doi.org/10.1017/SR18348>.
- Y. Wu, M. Li, F. Zhu, W. Hartley, J. Liao, W. An, S. Xue, J. Jiang, Variation on leaching behavior of caustic compounds in bauxite residue during dealkalization process, *J. Environ. Sci.* 92 (2020) 141–150, <https://doi.org/10.1016/j.jes.2020.02.004>.

- [37] K. Ramesh, L. Chen, F. Chen, Y. Liu, Z. Wang, Y.-F. Han, Re-investigating the CO oxidation mechanism over unsupported MnO, Mn<sub>2</sub>O<sub>3</sub> and MnO<sub>2</sub> catalysts, *Catal. Today* 131 (2008) 477–482, <https://doi.org/10.1016/j.cattod.2007.10.061>.
- [38] A. Majid, N. Ahmad, M. Rizwan, S.U. Khan, F.A.A. Ali, J. Zhu, Effects of Mn ion implantation on XPS spectroscopy of GaN thin films, *J. Electron. Mater.* 47 (2018) 1555–1559, <https://doi.org/10.1007/s11664-017-5955-1>.
- [39] P.N. Lemoungna, K. Wang, Q. Tang, X. Cui, Synthesis and characterization of low temperature (<800 °C) ceramics from red mud geopolymer precursor, *Constr. Build. Mater.* 131 (2017) 564–573, <https://doi.org/10.1016/j.conbuildmat.2016.11.108>.
- [40] W.C. Tang, Z. Wang, Y. Liu, H.Z. Cui, Influence of red mud on fresh and hardened properties of self-compacting concrete, *Constr. Build. Mater.* 178 (2018) 288–300, <https://doi.org/10.1016/j.conbuildmat.2018.05.171>.
- [41] A. Suss, A. Panov, A. Kozyrev, N. Kuznetsova, S. Gorbachev, Specific features of scandium behavior during sodium bicarbonate digestion of red mud, *Light Met.* 2018 (2018) 165–173, [https://doi.org/10.1007/978-3-319-72284-9\\_22](https://doi.org/10.1007/978-3-319-72284-9_22).
- [42] Z. Liu, H. Li, M. Huang, D. Jia, N. Zhang, Effects of cooling method on removal of sodium from active roasting red mud based on water leaching, *Hydrometallurgy* 167 (2017) 92–100, <https://doi.org/10.1016/j.hydromet.2016.10.021>.
- [43] N. Deihimi, M. Irannajad, B. Rezaei, Characterization studies of red mud modification processes as adsorbent for enhancing ferricyanide removal, *J. Environ. Manag.* 206 (2018) 266–275, <https://doi.org/10.1016/j.jenvman.2017.10.037>.
- [44] A.M. Ahamed, M.-N. Pons, Q. Ricoux, F. Goettmann, F. Lapique, Production of electrolytic iron from red mud in alkaline media, *J. Environ. Manag.* 266 (2020), 110547, <https://doi.org/10.1016/j.jenvman.2020.110547>.
- [45] H. Chen, J. Zheng, Z. Zhang, Q. Long, Q. Zhang, Application of annealed red mud to Mn<sup>2+</sup> ion adsorption from aqueous solution, *Water Sci. Technol.* 73 (11) (2016) 2761–2771, <https://doi.org/10.2166/wst.2016.139>.
- [46] I.V. Pekov, L.V. Olysysh, N.V. Chukanov, N.V. Zubkova, D.Y. Pushcharovsky, K. V. Van, G. Giester, E. Tillmanns, Crystal chemistry of cancrinite-group minerals with an AB-type framework: a review and new data. I. Chemical and structural variations, *Can. Mineral.* 49 (2011) 1129–1150, <https://doi.org/10.3749/canmin.49.5.1129>.
- [47] F. Xue, T. Wang, M. Zhou, H. Hou, Self-solidification/stabilisation of electrolytic manganese residue: mechanistic insights, *Constr. Build. Mater.* 255 (2020), 118971, <https://doi.org/10.1016/j.conbuildmat.2020.118971>.
- [48] X. Kong, T. Tian, S. Xue, W. Hartley, L. Huang, C. Wu, C. Li, Development of alkaline electrochemical characteristics demonstrates soil formation in bauxite residue undergoing natural rehabilitation, *Land Degrad. Dev.* 29 (2018) 58–67, <https://doi.org/10.1002/ldr.2836>.